High performance mode locking characteristics of single section quantum dash lasers

Ricardo Rosales

High performance mode locking characteristics of single section quantum dash lasers

Ricardo Rosales,[1,*] S. G. Murdoch,[2] R.T. Watts,[3] K. Merghem,[1] Anthony Martinez,[1] Francois Lelarge,[4] Alain Accard,[4] L. P. Barry,[3] and Abderrahim Ramdane[1]

[1]*CNRS, Laboratory for Photonics and Nanostructures, Route de Nozay, 91460 Marcoussis, France*
[2]*Physics Department, University of Auckland, Private Bag 92019, Auckland, New Zealand*
[3]*Research Institute for Networks and Communications Engineering, School of Electronic Engineering, Dublin City University, Dublin 9, Ireland*
[4]*III-V Lab, a joint Laboratory of "Alcatel Lucent Bell Labs" and "Thales Research & Technology" and CEA-LETI, Route de Nozay, 91460 Marcoussis, France*
[*]*ricardo.rosales@lpn.cnrs.fr*

Abstract: Mode locking features of single section quantum dash based lasers are investigated. Particular interest is given to the static spectral phase profile determining the shape of the mode locked pulses. The phase profile dependence on cavity length and injection current is experimentally evaluated, demonstrating the possibility of efficiently using the wide spectral bandwidth exhibited by these quantum dash structures for the generation of high peak power sub-picosecond pulses with low radio frequency linewidths.

OCIS codes: (250.0250) Optoelectronics; (140.0140) Lasers and laser optics; (140.5960) Semiconductor lasers; (140.4050) Mode-locked lasers.

References and links

1. M. J. Heck, E. J. Salumbides, A. Renault, E. A. Bente, Y. S. Oei, M. K. Smit, R. van Veldhoven, R. Nötzel, K. S. Eikema, and W. Ubachs, "Analysis of hybrid mode-locking of two-section quantum dot lasers operating at 1.5 microm," Opt. Express **17**(20), 18063–18075 (2009).
2. C. Y. Lin, Y. C. Xin, Y. Li, F. L. Chiragh, and L. F. Lester, "Cavity design and characteristics of monolithic long-wavelength InAs/InP quantum dash passively mode-locked lasers," Opt. Express **17**(22), 19739–19748 (2009).
3. L. Hou, M. Haji, J. Akbar, B. C. Qiu, and A. C. Bryce, "Low divergence angle and low jitter 40 GHz AlGaInAs/InP 1.55 μm mode-locked lasers," Opt. Lett. **36**(6), 966–968 (2011).
4. R. Rosales, K. Merghem, A. Martinez, A. Akrout, J.-P. Tourrenc, A. Accard, F. Lelarge, and A. Ramdane, "InAs/InP quantum-dot passively mode locked lasers for 1.55 μm applications," IEEE J. Sel. Top. Quantum Electron. **17**(5), 1292–1301 (2011).
5. K. Sato, "Optical pulse generation using Fabry-Pérot lasers under continuous-wave operation," IEEE J. Sel. Top. Quantum Electron. **9**(5), 1288–1293 (2003).
6. Y. Nomura, S. Ochi, N. Tomita, K. Akiyama, T. Isu, T. Takiguchi, and H. Higuchi, "Mode locking in Fabry-Perot semiconductor lasers," Phys. Rev. A **65**(4), 043807 (2002).
7. C. Gosset, K. Merghem, A. Martinez, G. Moreau, G. Patriarche, G. Aubin, A. Ramdane, J. Landreau, and F. Lelarge, "Subpicosecond pulse generation at 134 GHz using a quantum-dash-based Fabry-Perot laser emitting at 1.56 μm," Appl. Phys. Lett. **94**, 021107 (2009).
8. Z. G. Lu, J. R. Liu, S. Raymond, P. J. Poole, P. J. Barrios, and D. Poitras, "312-fs pulse generation from a passive C-band InAs/InP quantum dot mode-locked laser," Opt. Express **16**(14), 10835–10840 (2008).
9. H. A. Haus, "Mode-locking of lasers," IEEE J. Sel. Top. Quantum Electron. **6**(6), 1173–1185 (2000).
10. A. G. Vladimirov and D. Turaev, "Model for passive mode locking in semiconductor lasers," Phys. Rev. A **72**(3), 033808 (2005).
11. E. A. Viktorov, P. Mandel, A. G. Vladimirov, and U. Bandelow, "Model for mode locking in quantum dot lasers," Appl. Phys. Lett. **88**(20), 201102 (2006).
12. M. Radziunas, A. G. Vladimirov, E. A. Viktorov, G. Fiol, H. Schmeckebier, and D. Bimberg, "Pulse broadening in quantum-dot mode-locked semiconductor lasers: simulation, analysis and experiments," IEEE J. Quantum Electron. **47**(7), 935–943 (2011).
13. S. G. Murdoch, R. T. Watts, Y. Q. Xu, R. Maldonado-Basilio, J. Parra-Cetina, S. Latkowski, P. Landais, and L. P. Barry, "Spectral amplitude and phase measurement of a 40 GHz free-running quantum-dash modelocked laser diode," Opt. Express **19**(14), 13628–13635 (2011).

#158498 - $15.00 USD Received 21 Nov 2011; revised 2 Feb 2012; accepted 20 Feb 2012; published 29 Mar 2012

14. X. Tang, A. S. Karar, J. C. Cartledge, A. Shen, and G. H. Duan, "Characterization of a mode-locked quantum-dash Fabry-Perot laser based on measurement of the complex optical spectrum," Proc. 35th Eur. Conf. on Optical Commun. P2.21 (2009).
15. M. Bagnell, J. Davila-Rodriguez, A. Ardey, and P. J. Delfyett, "Dispersion measurements of a 1.3 μm quantum dot semiconductor optical amplifier over 120 nm of spectral bandwidth," Appl. Phys. Lett. **96**(21), 211907 (2010).
16. F. Lelarge, B. Dagens, J. Renaudier, R. Brenot, A. Accard, F. Dijk, D. Make, O. L. Gouezigou, J.-G. Provost, F. Poingt, J. Landreau, O. Drisse, E. Derouin, B. Rousseau, F. Pommereau, and G.-H. Duan, "Recent advances on InAs/InP quantum dash based semiconductor lasers and optical amplifiers operating at 1.55 μm," IEEE J. Sel. Top. Quantum Electron. **13**(1), 111–124 (2007).
17. D. A. Reid, S. G. Murdoch, and L. P. Barry, "Stepped-heterodyne optical complex spectrum analyzer," Opt. Express **18**(19), 19724–19731 (2010).
18. R. Maldonado-Basilio, J. Parra-Cetina, S. Latkowski, and P. Landais, "Timing-jitter, optical, and mode-beating linewidths analysis on subpicosecond optical pulses generated by a quantum-dash passively mode-locked semiconductor laser," Opt. Lett. **35**(8), 1184–1186 (2010).
19. A. Akrout, A. Shen, F. Lelarge, F. Pommereau, H. Gariah, F. Blache, G. H. Duan, and A. Ramdane, "Spectrum filtering and pulse compression of quantum-dash mode-locked lasers emitting at 1.55 mm," Proc. 34th Eur. Conf. on Optical Commun., P2.20 (2008).

1. Introduction

Semiconductor passively mode locked lasers (MLLs) are capable of emitting stable optical pulse trains in the absence of an external reference clock signal. Their compact size, ease of fabrication and low power consumption make them interesting for a variety of applications including high bit rate optical time division multiplexing, clock recovery and millimeter wave generation. These applications usually require specific mode locking (ML) characteristics, such as very short pulse widths with high peak powers and low radio frequency (RF) linewidths. Understanding, quantifying and being able to control these features is therefore of primary importance. Particularly in the 1.55 μm telecommunications window, there have been reports of quantum well and quantum dot mode locked lasers based on both the classical two-section configuration [1–4] and on the single section one devoid of a saturable absorber [5–8]. The physical mechanisms leading to the ML regime in two-section lasers are well understood [9–12], which facilitates the control of most of the ML characteristics, as opposed to the case of the single section devices. In this paper, a thorough characterization of single section quantum dash (QDash) based lasers as a function of cavity length and bias conditions is performed for the first time, which in combination with a simple theoretical analysis reveal interesting aspects for the understanding of this type of MLLs, allowing for the control of some of the important ML characteristics and for the achievement of high peak power sub-picosecond pulses at high repetition frequencies. A comparison of these devices with classical two-section MLLs based on the same QDash structures is also presented.

2. Theory

The complex electric field in a semiconductor passively MLL can be written as:

$$E(t)=\left[\sum_{n=1}^{N}E_n e^{j\left[\omega_n t+\theta_n(t)+\phi_n\right]}\right]+c.c \qquad (1)$$

where E_n, ω_n, $\theta_n(t)$ and ϕ_n are respectively the real amplitude, angular frequency, phase noise and static phase, of each of the N longitudinal modes. Under ML operation:

$$\frac{d}{dt}\left[\left(2\omega_{n+1}-\omega_n-\omega_{n+2}\right)t+2\theta_{n+1}(t)-\theta_n(t)-\theta_{n+2}(t)+2\phi_{n+1}-\phi_n-\phi_{n+2}\right]=0 \qquad (2)$$

for $n=1$ to $N-2$ and $N\geq 3$, which results in all the modes being phase correlated and equally separated, i.e.:

#158498 - $15.00 USD Received 21 Nov 2011; revised 2 Feb 2012; accepted 20 Feb 2012; published 29 Mar 2012

$$\theta_{n+1}(t) - \theta_n(t) = \Delta\theta(t) \tag{3}$$

$$\omega_{n+1} - \omega_n = \omega_r \tag{4}$$

with ω_r the angular repetition frequency such that the pulse train period $T = 2\pi / \omega_r$. The electric field intensity characterizing the MLL pulses can then be written as:

$$\begin{aligned} I(t) &\propto \left|E(t)\right|^2 \\ &= \sum_{m=1}^{N-1}\sum_{l=1}^{N-m} 2E_{m+l}E_l \cos\left[m\omega_r\left(t+\Delta t_r(t)\right) + \left(\phi_{m+l} - \phi_l\right)\right] + \sum_{m=1}^{N} E_m^2 \end{aligned} \tag{5}$$

with $\Delta t_r(t) = \Delta\theta(t)/\omega_r$ being the timing jitter of the generated pulses.

Besides Eqs. (3) and (4), the ML condition also implies that the relative phase:

$$\Psi(n) = 2\phi_{n+1} - \phi_n - \phi_{n+2} = \Phi_n \qquad \text{for } n \in [1, N-2] \tag{6}$$

with Φ_n being a constant. Moreover, the Φ_n should all have the same value and could be written without the subscript provided the total dispersion inside the laser cavity is independent of n throughout the entire pulse spectrum, as suggested from experimental work on different types of semiconductor lasers [5, 13–15]. Hence, by integrating Eq. (6) with respect to n one can find:

$$\int \Psi(n)dn = \phi_{n+1} - \phi_n = \Phi n + \alpha \qquad \text{for } n \in [1, N-1] \tag{7}$$

$$\int dn \int \Psi(n)dn = \phi_n = \Phi n^2/2 + \alpha n + \beta \qquad \text{for } n \in [1, N] \tag{8}$$

It can be seen from Eq. (8) that the ML condition imposes a quadratic evolution of the static phases ϕ_n as a function of mode number n whenever the value of $\Phi \neq 0$. For perfect pulse generation $\Phi = 2\pi m$, where m is any integer value, and in this case all modes interfere constructively. This is usually the case in classical two-section semiconductor passively MLLs as the absorber locks the static phases of the longitudinal modes by periodically creating a positive net gain window when saturated by the optical field inside the laser cavity. In single section or Fabry-Perot semiconductor lasers, other types of nonlinear processes in the gain medium, such as FWM, are able to set up a phase correlation among the modes which also become equally separated in frequency despite intracavity dispersion. This kind of ML mechanism has been experimentally observed for quantum well [5, 6], QDash [7] and quantum dot [8] based gain media. However, the phase correlation and the beating frequency locking in these devices come at the expense of a value of $\Phi \neq 0$, which will be determined by the nonlinear multi-wave parameters coupling the lasing modes [6]. This explains the usually high values of time bandwidth product (TBP) measured in single section mode locked lasers and, in some cases, the need of external dispersion compensation in order to obtain near transform limited pulses [5, 13]. Indeed, by making $d\omega = \omega_r dn$ in Eq. (7) and Eq. (8) and by considering only the second order term of the spectral phase ϕ_n, as the first and zero order terms do not affect the shape of $I(t)$, we can write:

$$\frac{d\phi(\omega)}{d\omega} = \Phi\omega/\omega_r^2 \tag{9}$$

$$\frac{d^2\phi(\omega)}{d\omega^2} = \Phi/\omega_r^2 \tag{10}$$

#158498 - $15.00 USD Received 21 Nov 2011; revised 2 Feb 2012; accepted 20 Feb 2012; published 29 Mar 2012

which are the group delay (GD) and the group delay dispersion (GDD), respectively, associated with the laser electric field inside the cavity. It can then be noted that the laser GDD could be compensated by e.g. the quadratic dispersion of fused silica in optical fibers by choosing the right length and dispersion sign. In this paper, after verification of the ML regime in the radio frequency domain, the GD and GDD have been measured for single section QDash MLLs as a function of cavity length and injection current. Low TBP and high peak power pulses were then obtained by means of dispersion compensation.

3. Device

The devices used for the experiments were single section QDash based lasers. The active region in these devices consists of nine layers of InAs QDashes separated by InGaAsP barriers [16]. Buried ridge stripe waveguide lasers were processed with a ridge width of 1.5µm. The as-cleaved lasers have a total length of ~890 and 1820 µm yielding repetition frequencies of ~48 and 23 GHz respectively, with threshold currents of 25 mA and 50 mA, and corresponding slope efficiencies of 0.13 W/A and 0.09 W/A per facet as shown in Fig. 1(a). Modal gain and internal losses were estimated at 50 cm^{-1} and 18 cm^{-1} respectively. These QDash based lasers also exhibit wide spectral features from which very short pulses could be generated provided the GDD is sufficiently small. Figure 1(b) illustrates the evolution of the spectral width at –3dB, which increases with injection current due to the band-filling effect.

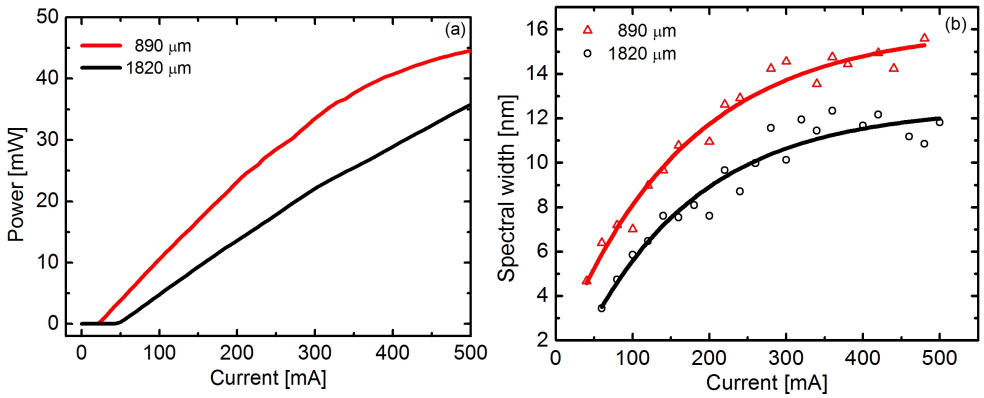

Fig. 1. (a) Light-current characteristics and (b) spectral width at –3dB of the QDash lasers.

4. Mode locking characteristics

Mode locking in both lasers was first analyzed by measuring their mode beatings in the RF domain in order to determine the ML range as a function of bias conditions. Figure 2(a) is the evolution of the RF linewidth for both lasers from 100 mA to 400 mA, reaching minimum values of 20 kHz (Fig. 2(b)) and 100 kHz (Fig. 2(c)), for the 890 and 1820 µm lasers respectively. These RF linewidths are narrow compared to the optical mode linewidths, which have been measured at ~10s of MHz by the self-heterodyne technique, confirming phase correlation between modes and hence the ML regime throughout the whole range of injection currents in both devices.

#158498 - $15.00 USD Received 21 Nov 2011; revised 2 Feb 2012; accepted 20 Feb 2012; published 29 Mar 2012

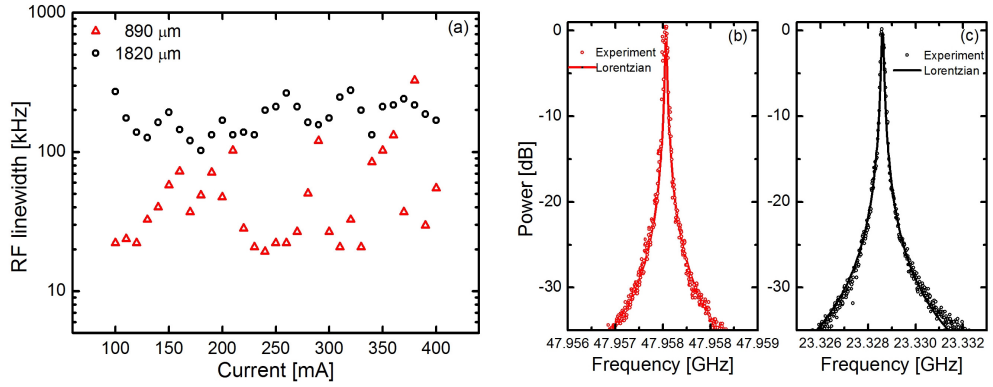

Fig. 2. (a) RF linewidth as a function of injection current and narrowest RF spectra for the (b) 890 μm and (c) 1820 μm long lasers.

The static phase difference $\phi_{n+1} - \phi_n$ between adjacent modes, up to a zero order term, were then measured for both lasers using the stepped heterodyne technique described in [17], from which the GD, GDD and spectral phase of the electric field have been determined. Figure 3(a) (red plot) is the measured GD for the 890 μm laser when biased at 400 mA as a function of offset frequency, spanning about 50 modes of the power spectrum (Fig. 3(b)). As expected from the ML condition (Eq. (9)), a linear GD is obtained, the slope of which determines the value of GDD which has been calculated at 1.3 ps^2. Figure 3(c) shows the corresponding spectral phase (red plot) obtained after integration of the GD curve, exhibiting the expected parabolic shape.

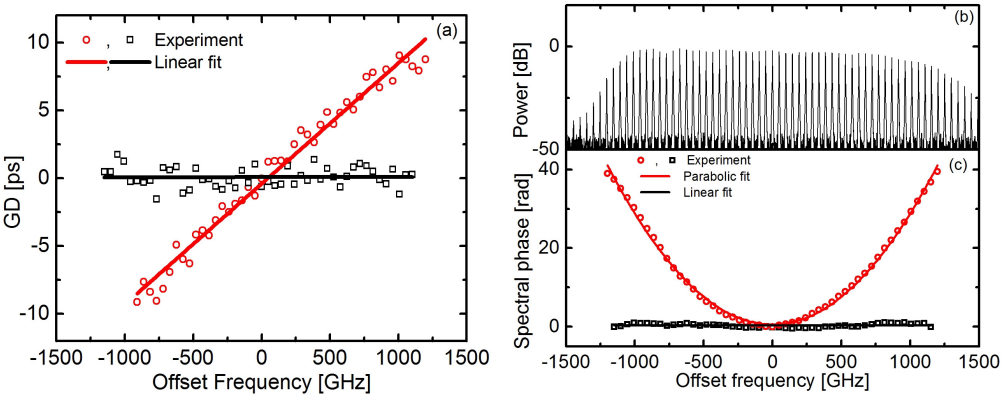

Fig. 3. (a) GD of the 890 μm laser measured at the laser output (red plot) and after 65 m of SMF (black plot) with corresponding (b) optical spectrum and (c) spectral phase at the laser output (red curve) and after 65 m of SMF (black curve) for an injection current of 400 mA.

Regardless of the perfect locking of the mode beating frequencies and the low RF linewidths, the parabolic spectral phase profile in Fig. 3(c) does not allow for pulse generation. In order to see this, the electric field intensity autocorrelation was measured directly from the laser by means of a second harmonic generation (SHG) background-free auto-correlator, as seen in the red curve of Fig. 4(a), showing an almost flat profile indicating the absence of sharp pulses, in agreement with the intensity profile in Fig. 4(b) (red curve), which has been reconstructed from the measured power and phase spectra. The previous measurements have been repeated after inserting 65 m of single mode fiber (SMF) at the laser output introducing –1.3 ps^2 of accumulated dispersion, which would compensate for the laser GDD of 1.3 ps^2. The black curves in Fig. 3(a) and Fig. 3(c) show the measured GD and the

#158498 - $15.00 USD Received 21 Nov 2011; revised 2 Feb 2012; accepted 20 Feb 2012; published 29 Mar 2012

spectral phase, respectively, after dispersion compensation. As can be noted, the second order term of the spectral phase is now negligible at the fiber end, where the modes now interfere constructively, allowing for perfect pulse generation. This is evidenced by the clean train of pulses in the intensity autocorrelation trace of Fig. 4(a) (black curve) which has been measured without using any type of optical amplification. In fact, the very narrow pulse widths, measured at 600 fs after deconvolution (assuming Gaussian pulse shape) and the 40 mW of average output power result in peak powers greater than 1 W, representing the highest peak power values ever obtained from a monolithic semiconductor mode locked laser emitting at 1.55 µm. The electric field intensity profile has once again been reconstructed and plotted in Fig. 4(b) (black curve) yielding 600 fs pulse widths in agreement with the measured autocorrelation trace, resulting in a TBP of 0.98.

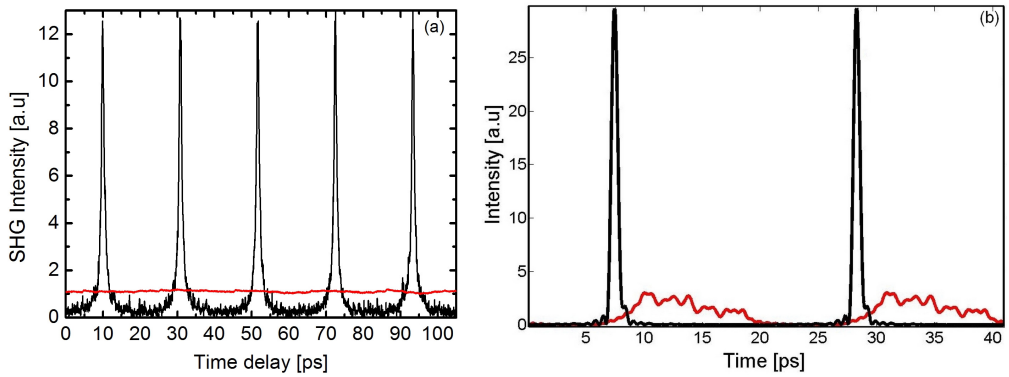

Fig. 4. (a) Intensity autocorrelation for the 890 µm laser at the laser output (red curve) and after 65 m of SMF (black curve) with corresponding (b) reconstructed field intensity profiles at the laser output (red curve) and after 65 m of SMF (black curve) when driven with 400 mA.

In order to see the effect of cavity length on the spectral phase, the same measurements were carried out for the 1820 µm long laser. Figure 5(a) is the plot of GD when the laser was biased at 400 mA. Figure 5(b) and Fig. 5(c) show respectively the measured power spectrum and spectral phase. The GDD was calculated at 3 ps^2, more than twice that of the shorter laser at the same bias current. Once again, this GDD was easily compensated by inserting 150 m of SMF at the laser output, allowing for the formation of 700 fs sharp pulses with a TBP of 0.97.

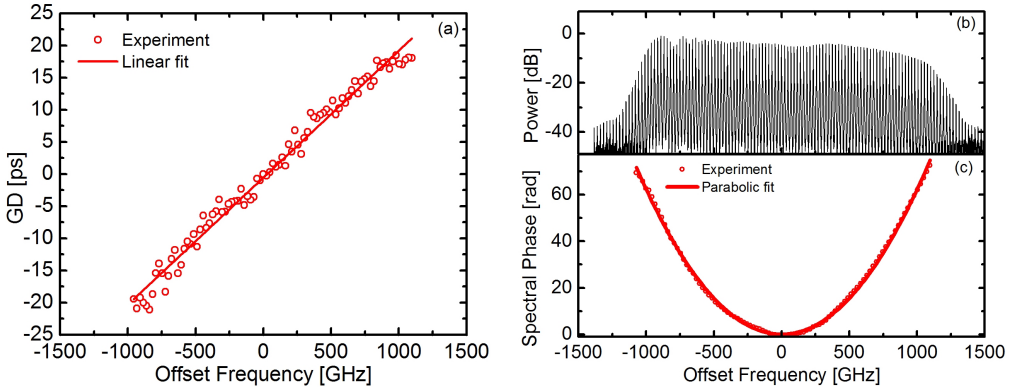

Fig. 5. (a) GD of the 1820 µm laser at the laser output with corresponding (b) optical spectrum and (c) spectral phase profile when driven with 400 mA.

To further investigate the GDD dependence on cavity length, GD measurements were performed for both lasers as a function of injection current. As expected, a linear GD curve was always obtained as the lasers were at all times under ML regime. Figure 6(a) shows the

#158498 - $15.00 USD Received 21 Nov 2011; revised 2 Feb 2012; accepted 20 Feb 2012; published 29 Mar 2012

evolution of measured GDD as a function of injection current for both lasers. Firstly, the GDD is found to decrease with current, suggesting that increased nonlinear effects favor the pulse formation in these structures, as also reported in [4, 18] where the pulse width was found to decrease when increasing the injection current. This represents an interesting feature in these MLLs as it allows for improving the pulse generation while increasing the average output power, contrary to classical two-section devices in which the shortest pulses are generally obtained at the lowest injection currents, yielding less average output power. Secondly, Fig. 6(a) shows that the GDD is always smaller for the shorter laser, in agreement with Eq. (10) stating that for the same value of Φ, a laser with longer cavity will exhibit higher dispersion, which can be intuitively understood as larger modal phase differences due to a longer propagation round-trip. The value of Φ is found to be slightly different in both lasers and to decrease with injection current from ~0.2 to ~0.1 rad. Despite these small values of Φ, pulses cannot be formed due to the relatively wide spectral widths if no dispersion compensation is performed. Indeed, the larger the spectral width the smaller the value of Φ or GDD required for pulse generation. This explains the observation of sharp pulses from single section semiconductor lasers only after filtering a few number of modes from the optical spectrum, as reported in [5, 19]. In order to see this, Fig. 6(b) illustrates the results of simulations showing the simultaneous effects of GDD and number of modes on pulse width for the 890 μm laser. A stronger dependence of GDD as the number of modes increases is clearly observed. For a small number of modes, the effect of GDD is less important as the mode phases will almost perfectly fit a straight line in which case the modes interfere constructively; however, as the number of modes increases, the modes will begin interfering out of phase due to accumulated dispersion, therefore affecting pulse generation leading to pulse broadening. At 400 mA, the number of modes at −3dB for this laser is ~30 from which a GDD = 1.3 ps^2 was measured. From Fig. 6(b), this yields a very broad intensity profile of ~9 ps with very low peak powers (as shown in Fig. 4(b)). In the case of zero GDD or, equivalently, after external dispersion compensation, pulse widths of ~600 fs are attainable, in agreement with the experimental results. In this case the pulse width will always decrease when increasing the number of modes as they will perfectly interfere in phase.

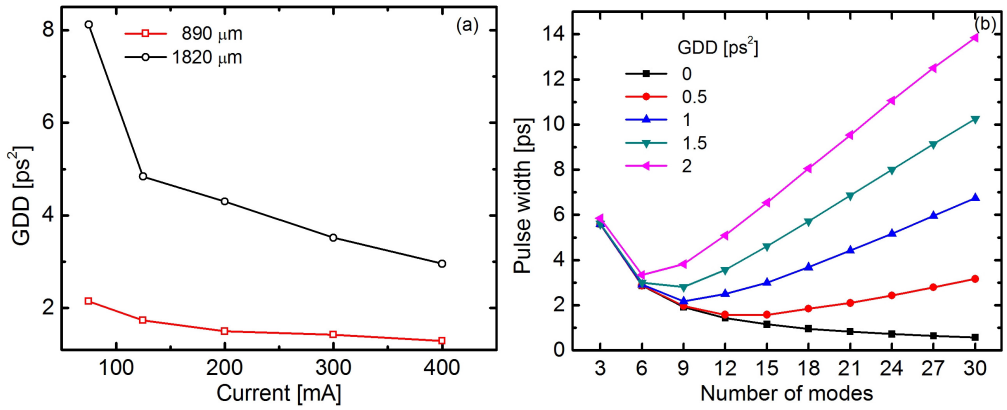

Fig. 6. (a) Measured GDD as a function of injection current for both lasers. (b) Calculated pulse width as a function of number of modes at −3 dB for different values of GDD for the 890 μm laser.

To compare the performance of the single section devices to that of a classical two-section MLL, the GD and GDD of a two-section laser including a saturable absorber have been measured. For comparison purposes, the two-section device comes from the same wafer and has exactly the same cavity length as the 48 GHz single section device previously characterized. The saturable absorber section has a length of 60 μm and the ML regime in this

#158498 - $15.00 USD Received 21 Nov 2011; revised 2 Feb 2012; accepted 20 Feb 2012; published 29 Mar 2012

laser is observed when this section is biased in the range between 0 and −3V depending on injection current. As in a classical passively MLL, the shortest pulses were obtained for the lowest currents and have been measured down to ~1 ps when driven with 70 mA in the gain section and −1.5 V of applied absorber bias, yielding an average power of ~4 mW. Under this bias condition, the GD was measured directly at the laser output as shown in Fig. 7, from which the GDD was estimated at 0.28 ps^2.

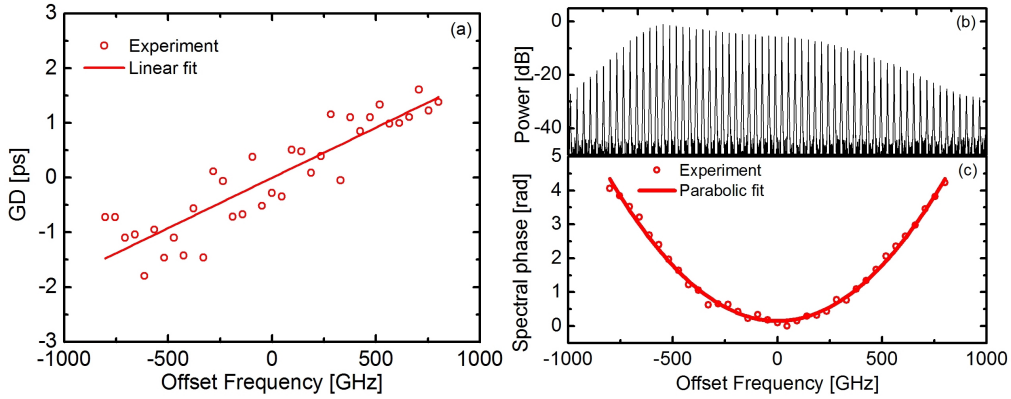

Fig. 7. (a) GD of the two-section 890 μm laser measured at the laser output with corresponding (b) optical spectrum and (c) spectral phase profile under 70 mA of injection current and −1.5 V of applied reverse bias.

As expected, both the GD and GDD were found to be much lower in the two-section device owing to the saturable absorber which periodically phase locks the longitudinal modes. The low GDD value is also evidenced by a clean autocorrelation trace (Fig. 8(a)) which is obtained without needing to insert additional SMF for dispersion compensation, and without resorting to optical amplification. The pulse widths were also measured from the reconstructed field intensity (Fig. 8(b)) and found to be 1.5 ps. The autocorrelation trace yields shorter pulses of 1.2 ps (after deconvolution) as a result of some GDD compensation due to −0.12 ps^2 of accumulated dispersion in our autocorrelation measurement setup. With a spectral width of 9.5 nm, the pulse TBP was calculated at 1.7, but could be reduced to the transform limited value by compensating the laser GDD as in the case for the 1-section devices. Two-section QDash passively MLLs hence exhibit a much lower GDD when compared to single section lasers having the same structure and cavity length; however, in order to obtain short pulses, the two-section device needs to be driven with high reverse absorber bias and low injection currents, which results in low average output powers. In addition, biasing the device at low gain currents does not allow to attain a wide spectral bandwidth, which increases with current (as shown in Fig. 1(b)), hence limiting the generation of shorter pulses. As a consequence, GDD compensated QDash single section MLLs are more advantageous than their two-section counterparts in terms of attainable power and pulse width.

#158498 - $15.00 USD Received 21 Nov 2011; revised 2 Feb 2012; accepted 20 Feb 2012; published 29 Mar 2012

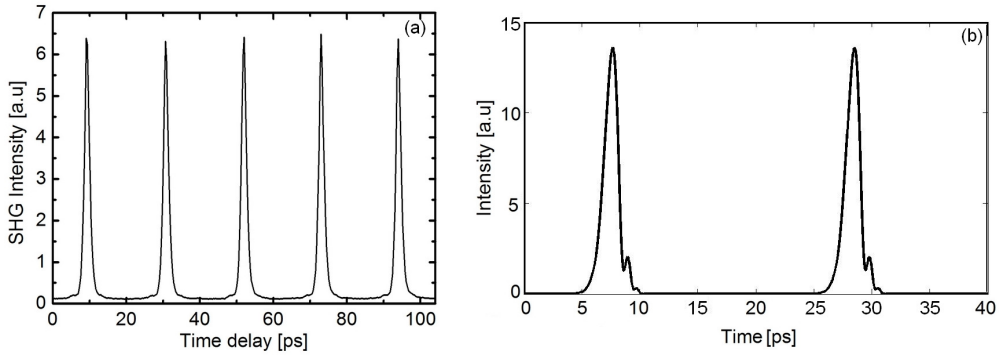

Fig. 8. (a) Intensity autocorrelation for the two-section 890 μm laser at the laser output with corresponding (b) reconstructed field intensity profile for an injection current of 70 mA and reverse bias of −1.5 V.

5. Summary

An analysis of the ML characteristics of single section QDash based lasers and a comparison with two-section devices have been presented. The experimental observations are in agreement with the ML condition relating the phases of the longitudinal modes. The GDD in the single-section devices was found to affect pulse generation but it proved to be easily compensated in order to efficiently use the wide spectral bandwidth attainable in these QDash structures for the generation of sub-picosecond pulses. Particularly, the GDD was found to decrease with injection current, favoring the formation of pulses while increasing the average output power, representing an advantage as compared to the classical two-section ML devices in which the shortest pulses are generally obtained at the lowest injection currents and under high reverse absorber bias, resulting in lower average output powers. Another interesting finding was the reduction of GDD with cavity length implying that ML pulses are more easily generated at higher repetition rates. Narrow RF linewidths in the single section devices of 10s to 100s of kHz were also measured, suggesting low phase noise of the laser intensity and hence relatively low timing jitter, which in combination with the very short pulses and high peak powers attainable in a wide range of repetition frequencies, demonstrate the high performance ML characteristics of single section QDash based lasers.

Acknowledgments

This work was supported by the French National Research Agency through the project TELDOT and by the Irish Higher Education Authority PRTLI programme through the INSPIRE project.

#158498 - $15.00 USD Received 21 Nov 2011; revised 2 Feb 2012; accepted 20 Feb 2012; published 29 Mar 2012